

## Thermomechanical parametric studies on residual stresses in S355 and S690 welded H-sections

Xiao Liu <sup>1,2</sup>, Kwok-Fai Chung <sup>1,2\*</sup>, Mingxin Huang <sup>3</sup>, Guodong Wang <sup>4</sup> and David A Nethercot<sup>1,5</sup>

<sup>1</sup>*Department of Civil and Environmental Engineering,  
The Hong Kong Polytechnic University, Hong Kong SAR, China.*

<sup>2</sup>*Chinese National Engineering Research Centre for Steel Construction (Hong Kong Branch)  
The Hong Kong Polytechnic University, Hong Kong SAR, China.*

<sup>3</sup>*Department of Mechanical Engineering, The University of Hong Kong, Hong Kong SAR, China.*

<sup>4</sup>*The State Key Laboratory of Rolling and Automation, Northeastern University, China.*

<sup>5</sup>*Department of Civil and Environmental Engineering, Imperial College London, U.K.*

*\* Corresponding author: kwok-fai.chung@polyu.edu.hk*

### ABSTRACT

In order to examine and compare welding-induced residual stresses in welded H-sections of different steel grades and heat input energy, extensive parametric studies were carried out using fully calibrated and highly efficient finite element models to perform coupled thermomechanical analyses. Numerical results including temperature history and distributions, residual stress distributions and magnitudes, and force equilibrium were discussed, and comparisons were made between calibrated finite element models with different steel grades, and different heat input energy during welding.

It was established that the residual stresses in S690 welded H-sections were proportionally less pronounced when compared with those in S355 welded H-sections of similar dimensions. Residual stresses in multi-pass S355 and S690 welded H-sections were shown to be significantly reduced, when compared with those in single-pass welded H-sections of similar dimensions. A simplified pattern was proposed to describe both the distributions and the magnitudes of residual stresses, and a set of formulae was also provided. It was confirmed that the residual stress pattern given in a definitive ECCS document for S355 sections was very conservative, and applicability of that pattern to S690 welded H-sections would significantly over-estimate residual stresses in these S690 sections. Hence, the proposed residual stress pattern together with the set of formulae for both S355 and S690 welded H-sections with single-pass and multi-pass welding should be adopted for accurate prediction of their structural behaviour.

**Keywords:** High strength steel; welding; coupled thermo-mechanical analysis; heat input energy; residual stresses patterns.

## **1. Introduction**

In general, large residual stresses are often induced in steel sections during fabrication, in particular, welding. The presence of these residual stresses will cause early material yielding, and thus, softening in these sections, and their adverse effects on both cross-sectional and member resistances should be properly allowed for in structural design (Willms, 2009). Welded H-sections are widely employed as structural members in steel structures, and hence, it is important to estimate both distributions and magnitudes of welding-induced residual stresses in these welded H-sections.

In the 1960s, many researchers investigated both distributions and magnitudes of residual stresses in welded H-sections made of S235 to S355 steel materials (McFalls and Tall, 1967; Kishima et al, 1969). A simplified residual stress pattern for welded H-sections was given in an ECCS document (1976), and then, it was modified in a revised version of the ECCS document (1984). This simplified pattern was widely adopted since then, and it was also incorporated into a number of modern structural design codes (SPC, 2003; CEN, 2005; AISC, 2016). This simplified pattern was considered to be well applicable for S355 welded H-sections, but its application to S690 welded H-sections had not been confirmed yet.

In this paper, the effects of welding-induced residual stresses in the high strength S690 steel welded H-sections are considered, and both distributions and magnitudes of welding-induced residual stresses in these welded H-sections will be established. Moreover, it is important to examine the effects of steel grades and heat input energy during welding in these welded H-sections, and it is highly desirable to establish a simplified residual stress pattern for these welded H-sections.

In general, quenching and tempering is one of the most commonly used methods to produce high strength S690-QT steel materials, and this heat treatment process is important for these steel materials to attain their enhanced mechanical properties. However, a heating / cooling cycle induced during welding may initiate phase transition, re-crystallization and grain growth in microstructures of these steel materials if both the heat input energy during welding and the cooling rate after welding are not properly controlled. Hence, significant reduction in mechanical properties of these welded sections, in particular, their heat affected zones, had been clearly identified because of changes in microstructures (Jenney and O'Brien, 2001). Moreover, such changes in microstructures in high strength S690 steel welded sections had been investigated and reported in the literature (Mayr, 2007; Ding et al., 2017; Azhari et al., 2018). However, it should be noted that this is outside the scope of the present investigation.

### **1.1 Effects of steel grades on residual stress patterns**

In the recent years, a number of experimental and numerical studies on structural behaviour of high strength S460 to S690 steel members were reported in the literature. Many researchers (Rasmussen

& Hancock, 1995; Lee et al, 2012; Wang et al, 2012; Masubuchi, 2013; Ban et al., 2013) conducted experiments to measure residual stresses in welded H- and box-sections, and to examine their effects on structural behaviour of these sections. According to their findings, the simplified residual stress pattern adopted in the ECCS document (1984) was generally considered to be too conservative for S690 welded H-sections as the amount of the steel materials yielded due to effects of welding was substantially smaller than those in S355 welded steel H-sections.

## **1.2 Effects of heat input energy on residual stress pattern**

With recent advances in computational heat transfer analyses, calibrated finite element models are readily employed to investigate and predict both distributions and magnitudes of welding-induced residual stresses in welded sections under different welding conditions (Fu et al., 2014). Many research reports on numerical investigations into residual stresses in welded sections with different heat input energy were reported in the past 10 years. Gery et al. (2005) conducted a numerical parametric study on the effects of welding speed, heat input energy, and heat source area onto temperature variations in butt-joint welding using three dimensional heat transfer models. It was found that an increase in the welding speed and the heat source area, or a decrease in the heat input energy would cause apparent decreases in the temperatures of the butt-joints. In 2011, Jiang et al. (2011) investigated the effects of different heat input energy and number of welding passes on residual stresses in a stainless steel clad plate using two dimensional models. It was found that when the heat input energy was decreased from 1.2 to 0.96 kJ/mm, longitudinal residual stresses in the steel plate were typically reduced by about 20% while the maximum residual stresses were decreased by about 10% when 4 welding passes were adopted instead of only 2. Fu et al (2016) established a number of three dimensional thermomechanical finite element models, and it was found that the welding procedures had significant influences on both the distributions and the magnitudes of residual stresses and distortions in fillet-welded T-joints.

## **1.3 Related experimental and numerical investigations on residual stresses**

A comprehensive experimental and numerical investigation into welding-induced residual stresses in welded H-sections was reported in a reference paper (Liu & Chung, 2018) published by the first two authors, and a total of four S690 steel welded H-sections with different cross-sectional dimensions were studied. Surface temperatures of the flanges of these sections were measured continuously using thermocouples during welding while surface residual stresses of both the flanges and the webs of these sections were measured using a hole drilling method after welding (Liu & Chung, 2016a). Moreover, advanced coupled thermomechanical analyses on three dimensional finite element models were carried out, and these models had been calibrated successfully after detailed comparison with measured data of both temperatures and residual stresses (Liu & Chung, 2016b). It should be noted that the measured and the predicted results of both temperatures and residual stresses reported in the

reference paper will be adopted for validation of the proposed two dimensional finite element models presented in Section 2.

#### **1.4 Objectives and scope of work**

Despite availability of calibrated three dimensional finite element models for coupled thermomechanical analyses reported in the reference paper (Liu & Chung, 2018), these three dimensional models always require huge demands on computational resources and time. It is a formidable work to complete a comprehensive numerical investigation using these three dimensional models (Duranton et al, 2004; Gery et al, 2005) to generate sufficient data and hence understandings on residual stress patterns of both S355 and S690 welded H-sections. It is highly desirable to establish highly efficient two dimensional finite element models which are able to give adequately accurate results of coupled thermomechanical analyses on welded H-sections with reduced computational resources and time.

Consequently, a comprehensive numerical investigation into thermal and mechanical responses in both S355 and S690 steel welded H-sections using two dimensional finite element models was undertaken, and the investigation took the following forms of activities:

##### **Task A Validation of a two dimensional finite element model**

Two dimensional finite element models for coupled thermomechanical analyses on welded H-sections are established, and they are carefully calibrated against both measured and predicted results of temperatures and residual stresses reported in the reference paper (Liu & Chung, 2018). It is important to demonstrate that these two dimensional models are capable to predict accurately both thermal and mechanical responses of welded H-sections with a high computational efficiency for subsequent parametric studies.

##### **Task B Parametric studies with different steel grades and heat input energy**

Using the two dimensional finite element models calibrated in Task A, systematic coupled thermomechanical analyses on both S355 and S690 welded H-sections with different cross-sectional dimensions are carried out as follows:

- Task B1  
Numerical analyses on welded H-sections with two different steel grades, namely, i) S355, and ii) S690, are carried out to determine both welding-induced temperatures and residual stresses for direct comparison.
- Task B2

Numerical analyses on both S355 and S690 welded H-sections with different heat input energy are carried out to determine both distributions and magnitudes of welding-induced residual stresses.

The areas of interest of the present investigation are:

- predicted residual stress patterns and their maximum values in both S355 and S690 welded H-sections with typical cross-sectional dimensions;
- comparison between the residual stress patterns given in the ECCS document (1984) and the predicted residual stress patterns for both S355 and S690 welded H-sections; and
- relationships between the maximum residual stresses in both S355 and S690 welded H-sections and the magnitudes of heat input energy adopted during welding.

Finite element models are established using ABAQUS 6.12 (2009) for a total of four welded H-sections with different cross-sectional dimensions, namely, Sections C1 and C4 as shown in Figure 1. It should be noted that various thermal properties of the steel materials at elevated temperatures given in EN1993-1-2 (2005) are adopted in these models to perform coupled thermomechanical analyses. Moreover, measured stress-strain curves of both S355 and S690 steel materials (Liu & Chung, 2018) plotted in Figure 2 are adopted for analyses of these Sections in Task A to give predicted residual stresses for comparison with measured values. However, bi-linear stress-strain curves are adopted in subsequent parametric analyses in Task B to give predicted residual stresses for development of generic residual stress patterns. While coupled thermomechanical analyses on all these four sections are performed successfully, numerical results of only Section C3 are illustrated in details owing to page limitation.

## **2. Validation of Two Dimensional Finite Element Models**

In order to develop highly efficient two dimensional finite element models to perform extensive parametric studies, two dimensional plane strain models are established for welded H-sections, namely, Sections C1 to C4, and coupled thermomechanical analyses on these sections are performed to predict both temperatures and residual stresses within the cross-sections of these welded H-sections (Liu, 2017). Owing to availability of the three dimensional finite element models described in Liu & Chung (2018) which have been calibrated thoroughly against measured data, their predicted results of temperatures and residual stresses of welded H-sections were adopted for calibration of the proposed two dimensional finite element models. Furthermore, various parameters for the coupled thermomechanical analyses in these three dimensional models are adopted in the proposed two dimensional models, and these include physical, thermal and mechanical properties of the steel materials at elevated temperatures given in EN1993-1-2 (2005) together with relevant thermal and mechanical boundary conditions. Both the two and the three dimensional models presented in this section adopt the measured engineering stress-strain curves in order to predict accurate residual

stresses. The measured engineering stress-strain curves of the S355 and the S690 steel materials are transformed into true stress-strain curves through the following equations:

$$\varepsilon_t = \ln ( 1 + \varepsilon ) \quad (1a)$$

$$\sigma_t = \sigma ( 1 + \varepsilon ) \quad (1b)$$

where

$\varepsilon$  and  $\varepsilon_t$  are the engineering and the true strains of the steel materials, and  
 $\sigma$  and  $\sigma_t$  are the engineering and the true stresses of the steel materials.

## 2.1. Finite element type and mesh

Figure 3 illustrates a typical three dimensional model adopted in Liu & Chung (2016b, 2018) together with a simplified two dimensional model proposed in this present investigation. The two dimensional models are established using a quadrilateral 4-noded generalized plane-strain element CPEG4T which is capable to carry out highly efficient non-linear analyses to calculate temperature rises and residual stresses. With a reference point, this element is able to simulate thermal expansion in the welding direction, i.e. the out-of-plane direction, making it applicable to compute residual strains and stresses in this direction. Thermal boundary conditions are shown in Figure 3 with specific values of the convection parameter and the emissivity value adopted in the thermal analyses.

It should be noted that a comprehensive study had been conducted to confirm mesh convergence of the three dimensional model in terms of both predicted temperatures and residual stresses (Liu & Chung, 2018). Hence, the same cross-sectional mesh configuration is adopted in the proposed two dimensional model in order to achieve the same degree of accuracy in the predicted values. In addition, local mesh refinement is adopted in the proposed two dimensional model in order to reduce element numbers and improve computational efficiency. As the welding-induced residual stresses in the flange-web junctions of the two dimensional model are expected to have large variations, fine meshes are provided in these regions locally. On the contrary, coarse meshes are provided in the regions far away from the flange-web junctions as variations in the residual stresses at these regions are expected to be small.

It should also be noted that tack welds are often provided in practice to hold both the flange and the web plates together in order to minimize any thermal distortion between them during welding. This is readily achieved in the proposed two dimensional model when plane strain elements are adopted together with relevant thermal and mechanical boundary conditions.

## 2.2. Heat source

As the double ellipsoidal model (Goldak et al., 1984 & 2006) widely adopted as a heat source, such as a welding arc, in three dimensional finite element models is not applicable in the proposed two dimensional models, a ramp model (Brown and Song, 1992) is proposed to simulate a moving heat source. It should be noted that the moving action is achieved by adjusting the level of the heat input energy,  $q$ , of the ramp model according to the following stages at different times,  $t_i$ , as shown in Figure 4:

- Stage 1: The heat source starts entering into the model:  
 $t_1 = 0$  ;                       $q_1 = 0$ ;
- Stage 2: The heat source arrives at another end of the model:  
 $t_2 = T / v$  ;                       $q_2 = q$  ;
- Stage 3: The heat source starts leaving the model:  
 $t_3 = T_{hs} / v$  ;                       $q_3 = q$ ,
- Stage 4: The heat source passes through the model completely:  
 $t_4 = (T_{hs} + T) / v$  ;       $q_4 = 0$ .

where

$T$  is the thickness of the model (mm);

$T_{hs}$  is the length of the heat source (mm);

$q$  is the heat input energy (kJ/mm);

$$= \eta U \times I / v$$

$\eta$  is the welding efficiency, and its value ranges from 0.85 to 0.95 for different welding methods;

$U$  is the voltage of the welding arc (V);

$I$  is the current of the welding arc (A); and

$v$  is the welding speed (mm/s).

The proposed heat source is readily considered as a single welding run, and hence, multiple weld-runs are generally required to complete an entire fabrication process for welded H-sections in practice. Consequently, for welding simulation of a flange-web junction, two single welding runs, namely, Runs B1 and B2, as shown in Figure 5, are required to perform welding in each flange-web junction of a welded H-section.

In order to reduce the effects of heat input energy, and hence, the magnitude of welding-induced residual stresses, multi-pass welding is adopted in which the heat input energy for each individual weld pass is reduced significantly. In the present investigation, it is suggested to replace a single weld-run with 3 weld-runs of reduced sizes, i.e. a multi-pass welding with 3 passes, and hence, the heat energy input for each weld-run is merely only one third of that of the single pass welding.

### 2.3. Comparison on temperature history and residual stresses

Coupled thermomechanical analyses on two dimensional models of these four welded H-sections have been completed successfully while key numerical results of only Section C3 is fully presented owing to page limitation.

#### 2.3.1. Temperature distributions

Figure 5 plots the temperature history at the centre-line of the outer surface of the bottom flange of Section C3 predicted by both the three and the two dimensional models. It is shown that the temperature history predicted by these two models follow closely to each other over the entire welding process of Runs B1 and B2. The maximum temperatures predicted by the three and the two dimensional models are found to be 472 and 476 °C, respectively with a small discrepancy of merely 4 °C or 0.84 %.

#### 2.3.2. Residual stress distributions

Figure 6 presents a comparison on predicted residual stress distributions across the entire flange width of Section C3 obtained from those three and two dimensional models. It is found that both the tensile and the compressive residual stresses predicted with the two dimensional model compare well with those predicted by the three dimensional model as follows:

- For the inner surface of the bottom flange, the maximum tensile and the maximum compressive residual stresses predicted by the three dimensional models are found to be 902 and -142 N/mm<sup>2</sup> respectively while those residual stresses predicted by the two dimensional models are found to be 915 and -137 N/mm<sup>2</sup>. Hence, the discrepancies are found to be 13 and 5 N/mm<sup>2</sup>.
- For the outer surface of the bottom flange, the maximum tensile and the maximum compressive residual stresses predicted by the three dimensional models are found to be 338 and -154 N/mm<sup>2</sup> respectively while those residual stresses predicted by the two dimensional models are found to be 369 and -147 N/mm<sup>2</sup>. Hence, the discrepancies are found to be 31 and 7 N/mm<sup>2</sup>.

Table 1 summarizes the predicted maximum residual stresses at the outer surfaces of the flanges, both tensile and compressive, and the averaged values of the predicted residual stresses within the flange thicknesses of Sections C1 to C4. Comparison among these values of the four sections predicted with the three and the two dimensional models is shown to be highly acceptable.

#### 2.3.3. Force equilibrium

A typical distribution of both the tensile and the compressive forces due to residual stresses at different parts of a welded H-section is illustrated in Figure 7. By summing up these forces, force equilibrium in the cross-sections is established. Both the tensile and the compressive forces of all the four sections are summarized in Table 2. It is shown that the out-of-balance forces due to numerical



errors for Sections C1 to C4 with S690 steel materials predicted with the three dimensional models are shown to be -1, +7, +2 and -2 kN respectively. The corresponding values for Sections C1 to C4 predicted with the two dimensional models are shown to be +4, +1, +3 and +1 kN, respectively. As the total tensile (or compressive) forces of these sections range from 210 to 486 kN, the out-of-balance forces are shown to be very small. Hence, force equilibrium in all of these sections is successfully achieved.

#### 2.3.4. Efficiency

Table 3 summarizes the computing time of coupled thermomechanical analyses on S690 welded H-sections using the three dimensional and the two dimensional models. It should be noted that both models have been thoroughly calibrated, and they are able to provide adequately accurate results. Hence, it is apparent that the two dimensional models are able to achieve a remarkable increase in computational efficiency, that is, with a saving of at least 95% in the computing time when compared with those three dimensional models using typical modern desktop computers. Technical specifications of the desktop computer used in carrying out these analyses are also given in Table 3.

Consequently, the proposed two dimensional models have been demonstrated to be adequately accurate for engineering application, and residual stress patterns in welded H-sections are readily obtained with these highly efficient two dimensional finite element models.

### 3. Parametric Studies

Extensive parametric studies have been carried out using the calibrated two dimensional finite element models to investigate effects of steel grades, and heat input energy on the residual stresses of the four welded H-sections. It should be noted that bi-linear stress-strain curves are adopted in subsequent parametric analyses in Task B in order to predict residual stresses for development of generic residual stress patterns. All the coupled thermomechanical analyses on these sections have been carried out successfully, and the numerical results are presented and discussed in the following sections.

#### 3.1. Effects of steel grades – S355 and S690 steel

A total of eight models of welded H-sections with four different cross-sectional dimensions, namely Sections C1 to C4, and two different steel materials, namely, S355 and S690, are established, and the programme of the parametric study is summarized in Table 4. It should be noted that all the welding parameters and all the thermal properties for these models with S355 and S690 steel are assigned to be the same (Liu, 2017) while the bilinear stress-strain curves illustrated in Figure 2 are adopted in the analyses.

### 3.1.1. Temperature distributions

Figure 8 plots typical predicted temperature history predicted with the two dimensional models of Sections C3 with S355 and S690 steel materials during the welding processes of Runs B1 and B2. It is shown that the predicted temperature history at the centre of the outer surfaces of the bottom flanges of Sections C3 with S355 and S690 steel materials are very close to each other, and the maximum discrepancy is found to be merely 5 °C.

Figure 9 illustrates the maximum temperature distributions of the flange-web junctions of the two dimensional models of Sections C3 with S355 and S690 steel materials at the end of each welding run of Runs B1 and B2. It is shown that large variations in temperatures exist within the sections, in particular, in the flange-web junctions, and very high temperatures exceeding 1500 °C have been predicted in the welded sections.

### 3.1.2. Residual stress distributions

Figure 10 illustrates both two and three dimensional plots of the predicted residual stresses of Sections C3 with S355 and S690 steel materials for direct comparison. The flange-web junction of Section C3 with S355 steel is shown to be almost completely yielded while only a small portion within the flange-web junction of Section C3 with S690 steel materials is yielded. It is also evident that the residual stress distribution in Section C3 with S690 steel materials are highly non-uniform within the plate thicknesses of both the flanges and the web. Consequently, it is established that, after averaging the residual stresses over the plate thickness, the average residual stresses in S690 welded H-sections are considerably smaller than those average residual stresses in S355 welded H-sections.

It should be noted that as each flange-web junction of Section C3 is fabricated with two welding runs, one at each side, i.e. Runs B1 and B2. A reduction in the residual stresses in the regions of the flange-web junction of the section caused by Run B1 is found after completion of Run B2. This stress reduction is widely believed to be caused by a ‘tempering effect’ of Run B2 acting onto the residual stresses induced by Run B1.

Table 5 summarizes the predicted maximum residual stresses at both the outer and the inner surfaces of the flanges, both tensile and compressive, together with the average values within plate thicknesses of the four sections with S355 and S690 steel materials. As expected, the residual stresses at the weld roots along the inner side of the flanges are very high, and they are found to range from 771 to 819 N/mm<sup>2</sup> for S690 welded H-sections, and from 381 to 388 N/mm<sup>2</sup> for S355 welded H-sections, owing to the presence of very high temperatures during welding. However, as the temperatures are significantly reduced across the plate thickness, the average residual stresses of the steel plates are found to be considerably smaller than the maximum values. More importantly, the averaged residual stresses in S690 welded H-sections are readily quantified to range from 420 to 538 N/mm<sup>2</sup>, i.e. smaller than the yield strength at 690 N/mm<sup>2</sup>. However, for S355 welded H-sections, the averaged residual stresses are found to range from 353 to 355 N/mm<sup>2</sup>, i.e. significant areas of the flange-web junctions

are yielded. Consequently, it is demonstrated that the effect of welding-induced residual stresses in S690 welded H-sections are proportionally less pronounced as these residual stresses are significantly smaller than the yield values of the steel plates. This is very different from those in S355 welded H-sections, and it is evident that significant yielding is found in the flange-web junctions of these H-sections.

It should be noted that all these residual stresses act along the longitudinal axes of the welded H-sections, and hence, they are out-of-plane stresses of the two dimensional models. Owing to high thermal stresses induced during welding, the steel materials in the vicinity of the weldment have been extensively yielded within the plane of the two dimensional cross-sections, and hence, their in-plane residual stresses are very high. In general, these in-plane residual stresses follow similar distributions of those of the out-of-plane residual stresses within the flange-web junctions.

### 3.1.3. Force equilibrium

By summing up residual stresses in various parts of each of the welded H-sections, various tensile and compressive forces in all the four sections are summarized in Table 6. It is shown that the out-of-balance forces due to numerical errors for Sections C1 to C4 with S355 steel materials predicted with the two dimensional models are shown to be +1, -2, -1 and -1 kN respectively. The corresponding values for Sections C1 to C4 with S690 steel materials are shown to be +4, +1, +3 and +1 kN, respectively. As the total tensile (or compressive) forces of these sections range from 166 to 486 kN, the out-of-balance forces are shown to be very small. Hence, force equilibrium in all of these sections is successfully achieved.

## 3.2. Effects of heat input energy: 0.35 to 2.0 kJ/mm

The parametric study on the effects of heat input energy on residual stresses in welded H-sections is summarized in Table 7, and Sections C1 to C4 with both S355 and S690 steel materials are covered in the study. As shown in Figure 11, the single pass welding in Section 3.1 are replaced with a multi pass welding with three welding runs, i.e. each of Runs B1 and B2 is divided into three runs, namely, Runs B1-1/2/3 and Runs B2-1/2/3, each with a reduced heat input energy. Hence, it should be noted that:

- a) For single-pass welding, the heat input energy for each of Runs B1 and B2 for Sections C1 and C2 is 1.05 kJ/mm while that for Sections C3 and C4 is 2.00 kJ/mm, as shown in Table 4.
- b) For multi-pass welding, the heat input energy for each of Runs B1-1/2/3 and B2-1/2/3 for Sections C1 and C2 is reduced to 0.35 kJ/mm while that for Sections C3 and C4 is 0.67 kJ/mm, as shown in Table 7.

The multi-pass welding is readily simulated with the use of a “birth and death” technique (ABAQUS, 2009).

### 3.2.1. Temperature distributions

Figure 12 plots typical predicted temperature history of the two dimensional models of Sections C3 with S355 and S690 steel materials during the welding processes of Runs B1-1/2/3 and B2-1/2/3. It is shown that the predicted temperature history at the centre of the outer surfaces of the bottom flanges of Sections C3 with S355 and S690 steel materials are very close to each other, and the maximum discrepancy is found to be merely 7 °C. For easy comparison, the corresponding temperature history of Sections C3 with Runs B1 and B2, i.e. single pass welding, are also plotted in Figure 12. It is shown that the maximum temperatures in Section C3 are decreased by about 113 °C.

Figure 13 illustrates the maximum temperature distributions of the flange-web junctions of the two dimensional models of Sections C3 with S355 and S690 steel materials at the end of each welding run of Runs B1-1/2/3 and B2-1/2/3. It is shown that large variations in temperatures exist within the sections, in particular, in the flange-web junctions, and very high temperatures exceeding 1500 °C have been predicted in the welded sections.

### 3.2.2. Residual stress distributions

Both two and three dimensional plots on the residual stress distributions of Sections C3 with S355 and S690 steel materials with multi-pass welding are presented in Figure 14. It is evident that the residual stress distributions of both S355 and S690 welded H-sections are highly non-linear, resulting in a highly non-uniform residual stress distribution within the flange-web junctions of the welded H-sections. When compared with the results of Sections C3 with a single-pass welding in Figure 10, it is found that:

- For S355 welded sections, only about one third of the flange-web junctions with multi-pass welding is yielded while extensive yielding is found in the flange-web junctions of S355 welded sections with single-pass welding.
- For S690 welded sections, significant reduction in the extent of yielding in the flange-web junctions with multi-pass welding was observed, when compared with that in the flange-web junctions with single-pass welding.

Hence, with a reduced heat input energy in each welding run, the magnitudes of the residual stresses are significantly reduced in both S355 and S690 steel welded H-sections. Moreover, it is established that the average residual stresses within plate thicknesses in both S355 and S690 welded H-sections with multi-pass welding are considerably smaller than those average residual stresses in welded H-sections with single-pass welding.

Table 8 summarizes the predicted maximum residual stresses at both the outer and the inner surfaces of the flanges, both tensile and compressive, together with the average values within plate thicknesses of the four sections with S355 and S690 steel materials. It is found that:

- For the inner surface of the bottom flange, the maximum tensile and the maximum compressive residual stresses predicted for S355 welded H-sections are found to be 456 and -77 N/mm<sup>2</sup> respectively while those residual stresses predicted for S690 welded H-sections are found to be 833 and -76 N/mm<sup>2</sup>.
- More importantly, the averaged residual stresses in S690 welded H-sections are readily quantified to range merely from 200 to 207 N/mm<sup>2</sup>, i.e. about 30% of the yield strength. Similarly, for S355 welded sections, the averaged residual stresses are found to range merely from 249 to 259 N/mm<sup>2</sup>, and they are about 70% of the yield strength.

Consequently, it is demonstrated that the welding-induced residual stresses in both S355 and S690 welded H-sections are significantly reduced when the heat input energy of each welding run is reduced.

### 3.2.3. Force equilibrium

By summing up residual stresses in various parts of each of the welded H-sections, various tensile and compressive forces in all the four sections are summarized in Table 9. It is shown that the out-of-balance forces due to numerical errors for Sections C1 to C4 with S355 steel materials predicted with the two dimensional models are shown to be +2, -1, +1 and 0 kN respectively. The corresponding values for Sections C1 to C4 with S690 steel materials are shown to be -2, -6, -1 and -1 kN, respectively. As the total tensile (or compressive) forces of these sections range from 91 to 290 kN, the out-of-balance forces are shown to be very small. Hence, force equilibrium in all of these sections is successfully achieved.

## 4. Simplified Residual Stress Patterns

Based on the results of the parametric studies, a simplified residual stress pattern for welded H-sections with different steel grades, and different heat input energy during welding is proposed after averaging their predicted residual stresses within plate thicknesses of the flanges and the webs. The proposed residual stress pattern is shown in Figure 15. As the proposed pattern represents directly the numerical results of the finite element analyses presented in Section 3, accuracy of the proposed pattern is well established according to the verification of the two dimensional finite element models presented in Section 2. A total of 4 parameters, namely,  $\alpha^+$ ,  $\alpha^-$ ,  $\beta^+$  and  $\beta^-$  are adopted to represent both the magnitudes and the distributions of the residual stresses, and they are defined as follows:

- $\alpha^+$  is the ratio of the maximum tensile residual stress in the flange,  $f_{rf}$ , divided by the yield strength of the steel plate,  $f_y$ ;
- $\alpha^-$  is the ratio of the maximum compressive residual stress in the flange,  $f_{rf}$ , divided by the yield strength of the steel plate,  $f_y$ ;

- $\beta^+$  is the ratio of the maximum tensile residual stress in the web,  $f_{rw}$ , divided by the yield strength of the steel plate,  $f_y$ ; and
- $\beta^-$  is the ratio of the maximum compressive residual stress in the web,  $f_{rw}$ , divided by the yield strength of the steel plate,  $f_y$ .

For direct comparison, the ECCS residual stress pattern recommended for S235 to S355 welded sections is also shown in Figure 15. It is evident that these two patterns are broadly similar in shape. Moreover, high tensile residual stresses exist at the flange-web junctions of both patterns, and they are readily balanced by relatively small compressive residual stresses over the rest of the flanges and the central portions of the webs.

In order to assess their relative residual stress levels, Table 10 summarizes all the residual stress ratios of both single-pass and multi-pass welded H-sections for direct comparison, and both S355 and S690 steel materials are considered. It is shown that:

#### Single-pass welding

- Comparison among the maximum ratios of  $\alpha^+$  and  $\alpha^-$  in the flanges of S355 and S690 Sections C1 and C2 shows that they decrease from +1.00 and -0.49 to +0.78 and -0.24 respectively.
- Similarly, comparison among the maximum ratios of  $\alpha^+$  and  $\alpha^-$  in the flanges of S355 and S690 Sections C3 and C4 shows that they decrease from +1.00 and -0.34 to +0.61 and -0.18 respectively.
- Similar results are found for the maximum ratios of  $\beta^+$  and  $\beta^-$  in the webs of S355 and S690 Sections C1 to C4.

#### Multi-pass welding

- Comparison among the maximum ratios of  $\alpha^+$  and  $\alpha^-$  in the flanges of S355 and S690 Sections C1 and C2 shows that they decrease from +0.73 and -0.24 to +0.30 and -0.12 respectively.
- Similarly, comparison among the maximum ratios of  $\alpha^+$  and  $\alpha^-$  in the flanges of S355 and S690 Sections C3 and C4 shows that they decrease from +0.70 and -0.20 to +0.29 and -0.10 respectively.
- Similar results are found for the maximum ratios of  $\beta^+$  and  $\beta^-$  in the webs of S355 and S690 Sections C1 to C4.

In general, it is expected that the maximum residual stresses, and the corresponding residual stress ratios both at the flange and at the web in the vicinity of the flange / web junctions,  $\alpha^+$  and  $\beta^+$ , should have the same values according to various established residual stress patterns on S355 welded sections. However, this is not applicable to S690 welded sections. It should be noted that:

- There are significant temperature variations across the flange thicknesses during welding, as shown in Figures 11 and 13 for single and multi-pass welding respectively, and hence, the

corresponding welding-induced strains in both the flanges and the webs in the vicinity of the flange /web junctions are normally not the same.

- For S355 welded sections, these strains, though different, are sufficiently large to cause full yielding of the steels in the junctions. Hence, the corresponding residual stresses are found to be equal to the yield strengths of the steels, and both  $\alpha^+$  and  $\beta^+$  are equal to 1.0, as shown in Figures 10a) and 14a) for single and multi-pass welding respectively.
- However, for S690 welded sections, despite the presence of large welding-induced strains in both the flanges and the webs in the vicinity of the flange/web junctions, these strains are not sufficiently large to cause full yielding in the steels, as shown in Figures 10b) and 14b). Owing to highly non-linear temperatures, and hence, residual stresses within the flange and the web thicknesses, it is necessary to take weighted averages of these stresses to obtain simplified residual stress patterns. Hence, after these calculations, the residual stress ratios for the flanges and the webs at the flange/web junctions,  $\alpha^+$  and  $\beta^+$ , are found to be not the same while force equilibrium is always achieved after summing up these averaged residual stresses over the entire cross-sections.

Consequently, it is shown that replacing single-pass welding with multi-pass welding in both S355 and S690 welded H-sections is highly beneficial as the maximum ratios for tensile and compressive residual stresses,  $\alpha^+$  and  $\alpha^-$ , in the flanges of these welded H-sections are demonstrated to be decreased by a factor of about 1.5 to 2.0. The same factors also apply to the maximum ratios for tensile and compressive residual stresses,  $\beta^+$  and  $\beta^-$ , in the webs of these welded H-sections.

For ease of presentation, all the values of the maximum residual stress ratios given in Table 10 may be readily evaluated with the set of formulae listed in Table 11 while limits of applicability on geometrical dimensions of these welded H-sections are also presented in Table 11.

## 5. Conclusions

Despite availability of calibrated three dimensional finite element models for coupled thermomechanical analyses reported in the complementary paper (Liu & Chung, 2018), these three dimensional models always require huge demands on computational resources and time. It is a formidable work to complete a comprehensive numerical investigation using these three dimensional models to generate sufficient data and hence understandings on residual stress patterns of both S355 and S690 welded H-sections. It is highly desirable to establish efficient two dimensional finite element models which are able to give adequately accurate results of coupled thermomechanical analyses on welded H-sections with reduced demands on computational resources and time.

Consequently, a comprehensive numerical investigation into thermal and mechanical responses in both S355 and S690 steel welded H-sections using two dimensional finite element models was

undertaken, and key findings of the parametric studies on these coupled thermomechanical analyses are summarized as follows:

- In general, yielding is extensive in the flange-web junctions in S355 welded H-sections, but it is rather restricted in those junctions in S690 welded H-sections. Consequently, it is established that the residual stresses in S690 welded H-sections are proportionally less pronounced when compared with those in S355 welded H-sections of similar dimensions.
- Compared with welded H-sections of single-pass welding, the extent of yielding in the flange-web junctions in those S355 and S690 welded H-sections with multi-pass welding is shown to be significantly reduced. Hence, it is established that the residual stresses in S355 and S690 welded H-sections with multi-pass welding are significantly reduced, when compared with those welded H-sections of similar dimensions with single-pass welding.
- A simplified pattern was proposed to describe both the distribution and the magnitude of residual stresses of welded H-sections, and a set of formulae was also provided. It was confirmed that the residual stress pattern given in the definitive ECCS document (1984) for S355 sections was very conservative, and applicability of this pattern to S690 welded H-sections would significantly over-estimate residual stresses in these S690 sections.

Hence, the proposed pattern together with the set of formulae for both S355 and S690 welded H-sections with single-pass and multi-pass welding should be adopted for accurate prediction of their structural behaviour. Applicability of the proposed residual stress patterns on welded H-sections with specific ranges of cross-sectional sizes was also provided.

## **Acknowledgement**

The project leading to publication of this paper is partially funded by the Research Grants Council of the Government of Hong Kong SAR (Project No. PolyU 5148/13E and PolyU 152194/15E) and the Research Committee of the Hong Kong Polytechnic University. The authors also wish to acknowledge the Chinese National Engineering Research Centre for Steel Construction (Hong Kong Branch) at the Hong Kong Polytechnic University for financial support (Project Nos. BBY3 and BBY6) to the project.

## **References**

- 1) Willms R (2009). High strength steel for steel construction. Proceedings of Nordic Steel Construction Conference, pp597-604.
- 2) McFalls RK and Tall L (1967). A study of welded columns manufactured from flame-cut plates. Master's thesis, Lehigh University.
- 3) Kishima Y, Alpsten G, and Tall L (1969). Residual stresses in welded shapes of flame-cut plates in ASTM A572 (50) steel. Fritz Eng. Lab. Rep. No. 321.2, Lehigh University, Bethlehem.



- 4) ECCS (1976). Manual on Stability of Steel Structures. European Convention for Constructional Steelwork Publication, 2<sup>nd</sup> Edition.
- 5) ECCS (1984). Manual on Stability of Steel Structures. European Convention for Constructional Steelwork Publication, 3<sup>rd</sup> Edition.
- 6) SPC (2003). GB/T 50017-2017: Code for design of steel structures (in Chinese). Standard Press of China, Beijing, China.
- 7) CEN (2005). EN-1993-1-1:2005, Eurocode 3: Design of steel structures – Part 1–1: General rules and rules for buildings. European Committee for Standardization, Brussels, Belgium.
- 8) CEN (2005). EN-1993-1-2:2005, Eurocode 3: Design of steel structures – Part 1–2: General rules—Structural fire design. European Committee for Standardization, Brussels, Belgium.
- 9) AISC (2016). ANSI/AISC 360-16: Specification for Structural Steel Buildings. American Institute of Steel Construction, Chicago, U.S.A.
- 10) Jenney CL, O'Brien A. (2001). Welding Handbook. Welding Science and Technology Vol. 1. American Welding Society.
- 11) Mayr P. (2007). Evolution of microstructure and mechanical properties of the heat affected zone in B-containing 9% chromium steels. PhD Thesis. Faculty of Mechanical Engineering, Graz University of Technology, Austria.
- 12) Ding Q, Wang T, Shi Z, Wang Q, Wang Q, and Zhang F. (2017). Effect of welding heat input on the microstructure and toughness in simulated CGHAZ of 800 MPa Grade steel for hydropower penstocks. *Metals*; 7(4):115.
- 13) Azhari F, Al-Amin Hossain A, Heidarpour A, Zhao XL, and Hutchinson CR. (2018). Mechanical response of ultra-high strength (Grade 1200) steel under extreme cooling conditions. *Constructional Building Materials*; 175:790–803.
- 14) Rasmussen K and Hancock G. (1995). Tests of high strength steel columns. *Journal of Constructional Steel Research*, 34(1): 27-52.
- 15) Lee CK, Chiew SP and Jiang J. (2012). Residual stress study of welded high strength steel thin-walled plate-to-plate joints. Part 1: Experimental study. *Thin-Walled Structures*, 56: 103-112.
- 16) Wang YB, Li GQ and Chen SW. (2012). Residual stresses in welded flame-cut high strength steel H-sections. *Journal of Constructional Steel Research*, 79: 159-165.
- 17) Masubuchi K. (2013). Analysis of welded structures: Residual stresses, distortion, and their consequences. Elsevier, vol. 33.
- 18) Ban, HY, Shi G, Bai Y, Shi YJ, and Wang Y. (2013). Residual stress of 460 MPa high strength steel welded I section: Experimental investigation and modelling. *International Journal of Steel Structures*, 13(4): 691-705.
- 19) Fu G, Lourenco MI, Duan M, and Estefen SF. (2014). Effect of boundary conditions on residual stress and distortion in T-joint welds. *Journal of Constructional Steel Research*, 102: 121-135.
- 20) Gery D, Long H, & Maropoulos P. (2005). Effects of welding speed, energy input and heat source distribution on temperature variations in butt joint welding. *Journal of Materials Processing Technology*, 167(2): 393-401.

- 21) Jiang WC, Wang BY, Gong JM, and Tu ST. (2011). Finite element analysis of the effect of welding heat input and layer number on residual stress in repair welds for a stainless steel clad plate. *Materials & Design*, 32(5), 2851-2857.
- 22) Fu G, Lourenço MI, Duan M, and Estefen SF. (2016). Influence of the welding sequence on residual stress and distortion of fillet welded structures. *Marine Structures*, 46: 30-55.
- 23) Liu X and Chung KF. (2016a). Experimental investigation into residual stresses of welded H-sections made of Q690 steel materials. *Proceeding of the Fourteenth East Asia-Pacific Conference*, Ho Chi Minh City, January 2016, pp559-566.
- 24) Liu X and Chung KF. (2016b). Numerical investigation into residual stresses of welded H-sections made of Q690 steel materials. *Proceeding of the Eleventh Pacific Structural Steel Conference*, Shanghai, October 2016, pp1205-1211.
- 25) Duranton P, Devaux J, Robin V, Gilles P and Bergheau JM. (2004). 3D modelling of multi-pass welding of a 316L stainless steel pipe. *Journal of Materials Processing Technology*, 153: 457-463.
- 26) Liu X. (2017). Structural effects of welding onto high strength S690 steel plates and welded sections. PhD Thesis, The Hong Kong Polytechnic University.
- 27) ABAQUS 6.12 (2009). Theory Manual. Providence, US: Dassault Systemes Simulia Corp., U.S.A.
- 28) Liu X, and Chung KF. (2018). Experimental and numerical investigation into temperature histories and residual stress distributions of high strength steel S690 welded H-sections. *Engineering Structures*, 165: 396-411.
- 29) Goldak JA, Akhlaghi M. (2006). *Computational Welding Mechanics*. Springer Science & Business Media.
- 30) Goldak J, Chakravarti A and Bibby M. (1984). A new finite element model for welding heat sources. *Metallurgical Transactions B*, 15(2), 299-305.
- 31) Brown S & Song H. (1992). Finite element simulation of welding of large structures. *Journal of Engineering for Industry*, 114(4): 441-451.

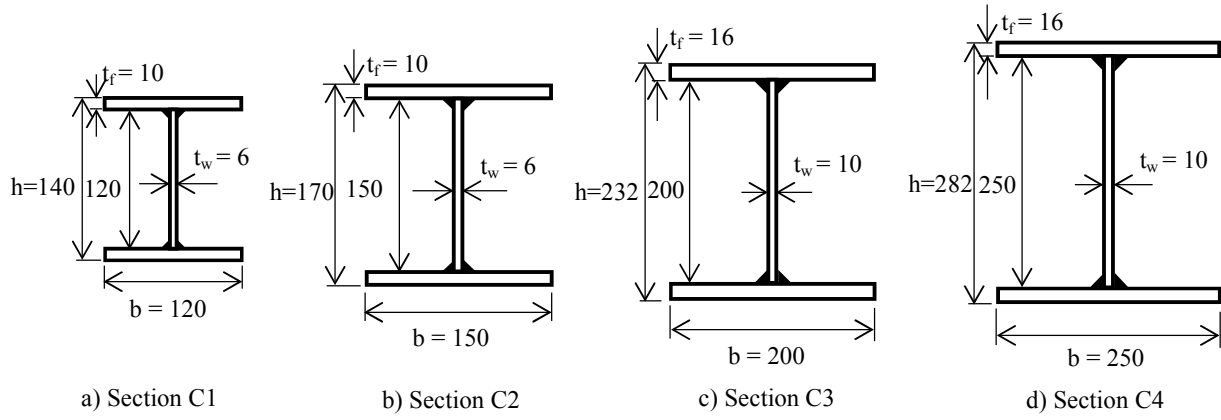


**Figure 1. Cross-sectional dimensions of four different welded H-sections**

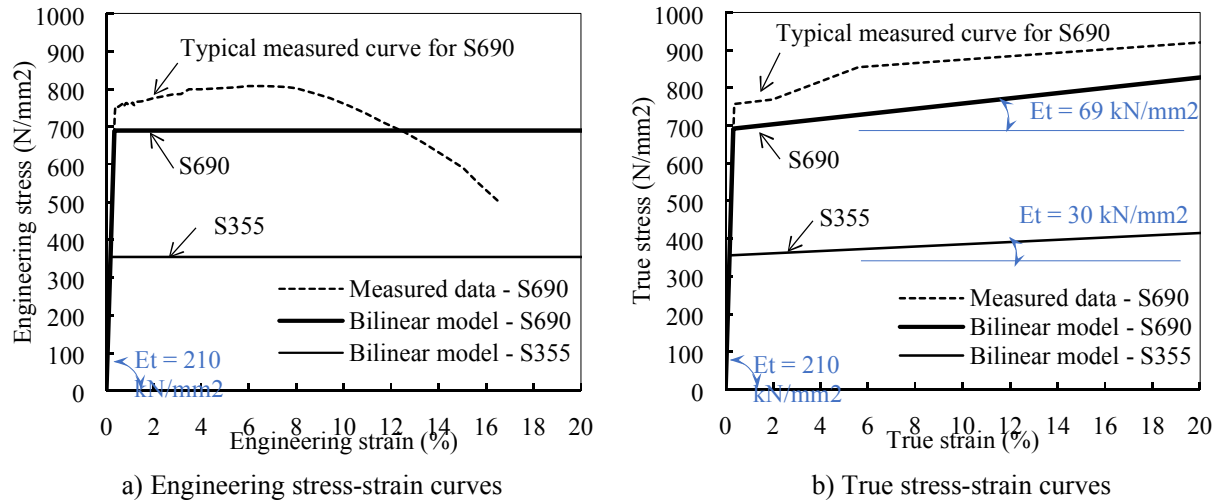


**Figure 2. Stress-strain curves adopted for S355 and S690 steel materials**

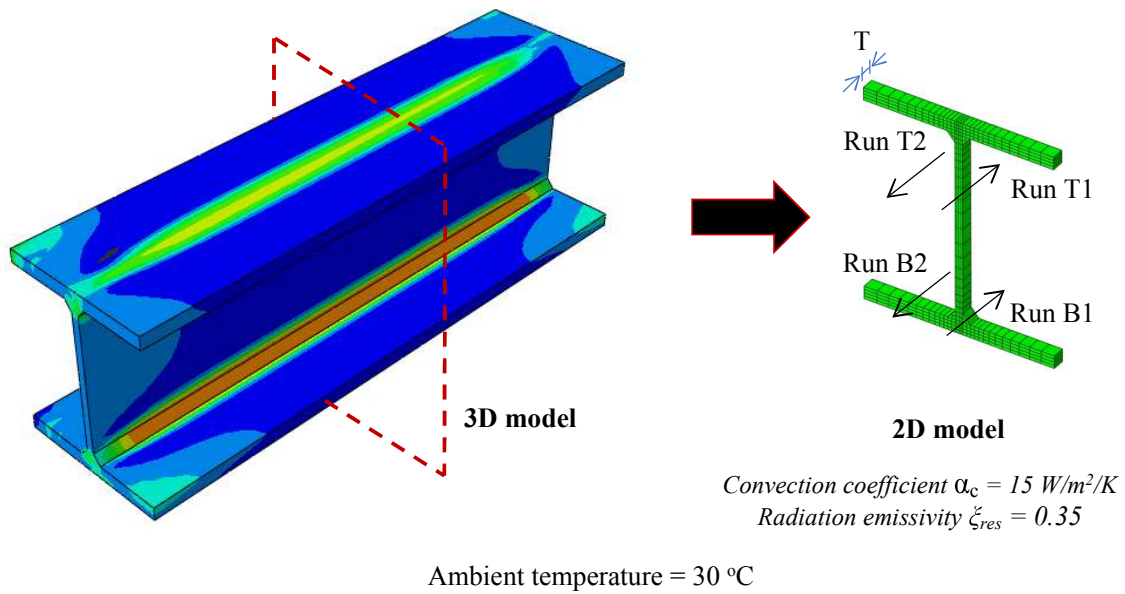


**Figure 3. Typical 3D and 2D models of welded H-sections undergoing coupled thermo-mechanical analyses**

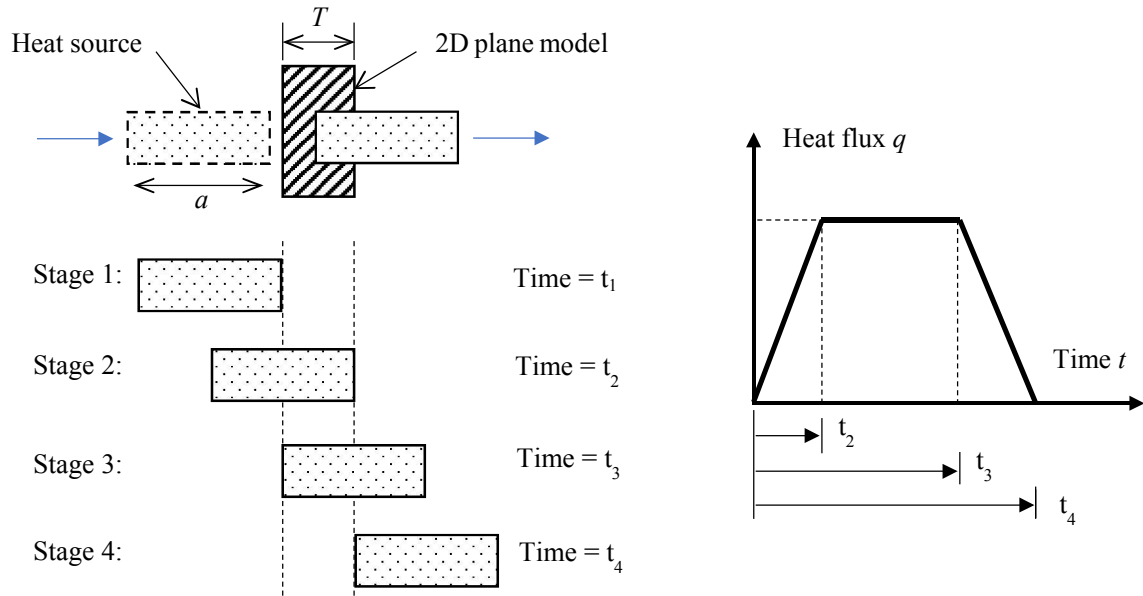


Figure 4. A ramp model as a heat source in 2D models

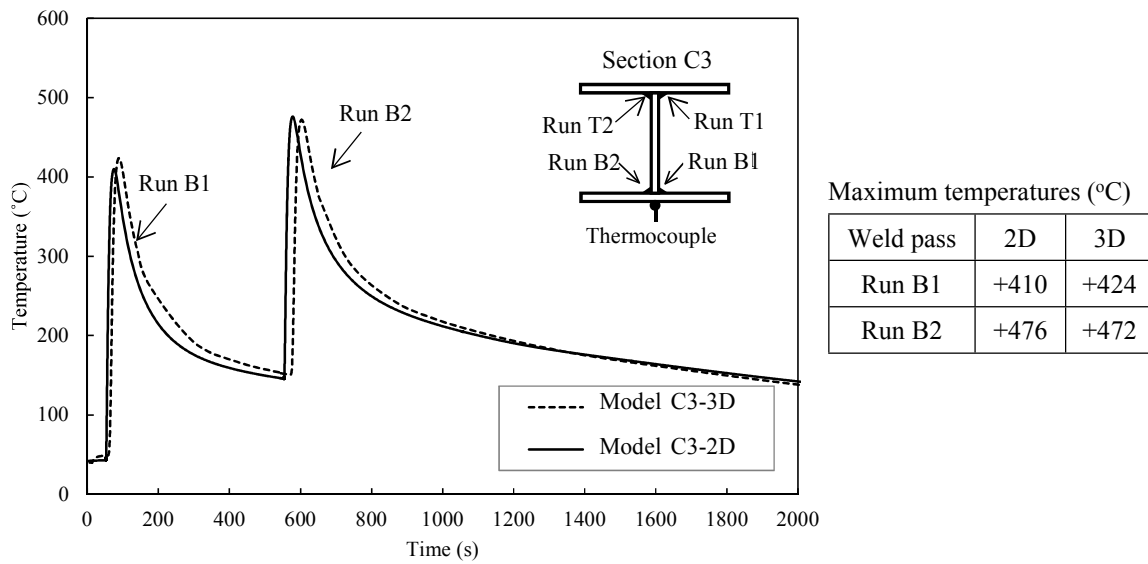
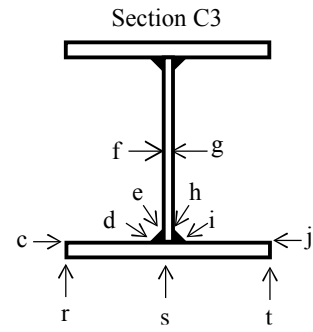
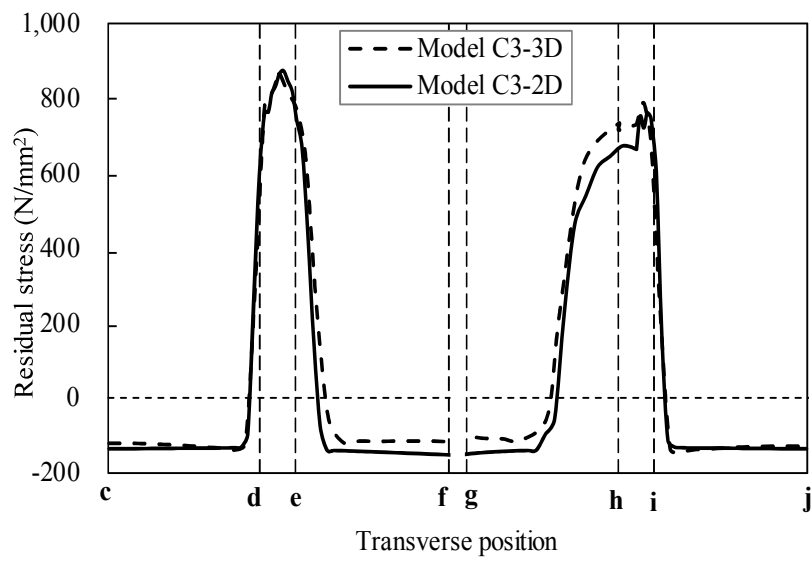
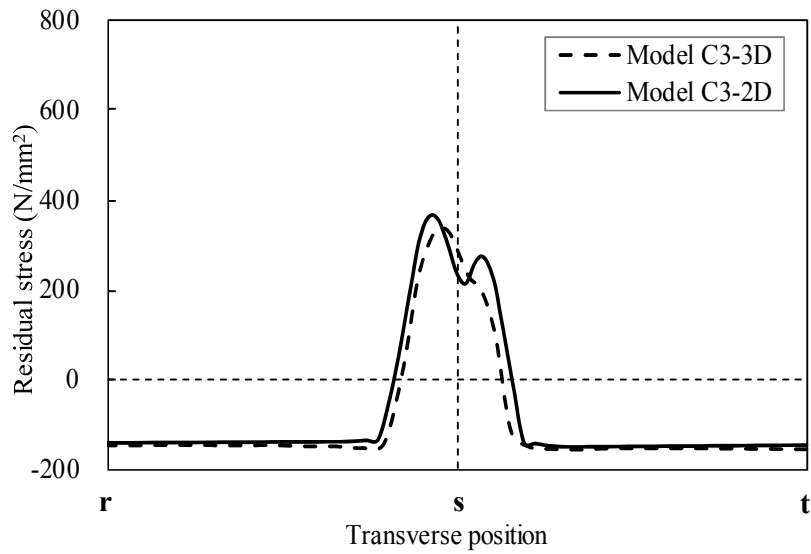


Figure 5. Typical predicted temperature history of 2D and 3D models of welded H-sections



Residual stresses

N/mm <sup>2</sup>	2D	3D
Tensile	+915	+902
Compression	-137	-142



Residual stresses

N/mm <sup>2</sup>	2D	3D
Tensile	+369	+338
Compression	-147	-154

Figure 6. Typical predicted residual stresses of 2D and 3D models of welded H-sections

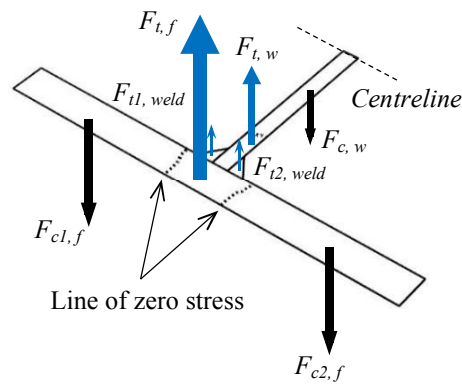
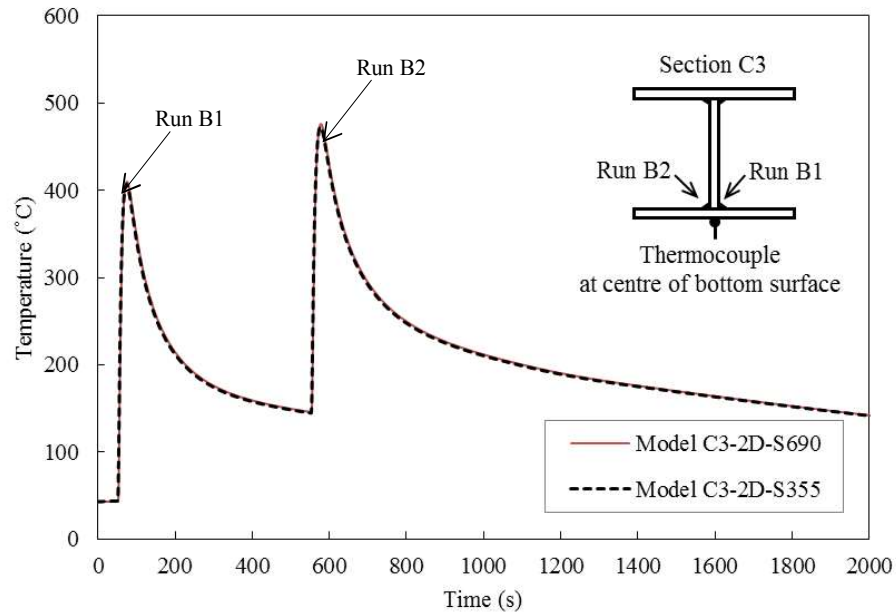
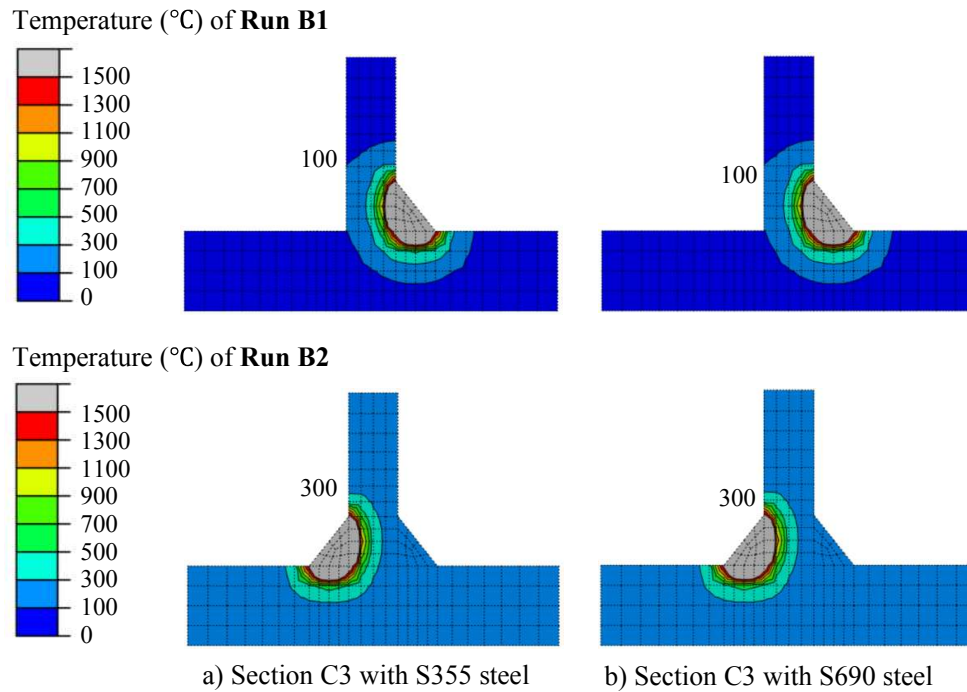


Figure 7. Tensile and compressive forces acting on a cross-section of a welded H-section



**Figure 8. Typical predicted temperature history of 2D models of S355 and S690 welded H-sections – Single pass welding**



**Figure 9. Predicted temperature distributions of 2D models of S355 and S690 welded H-sections – Single pass welding**

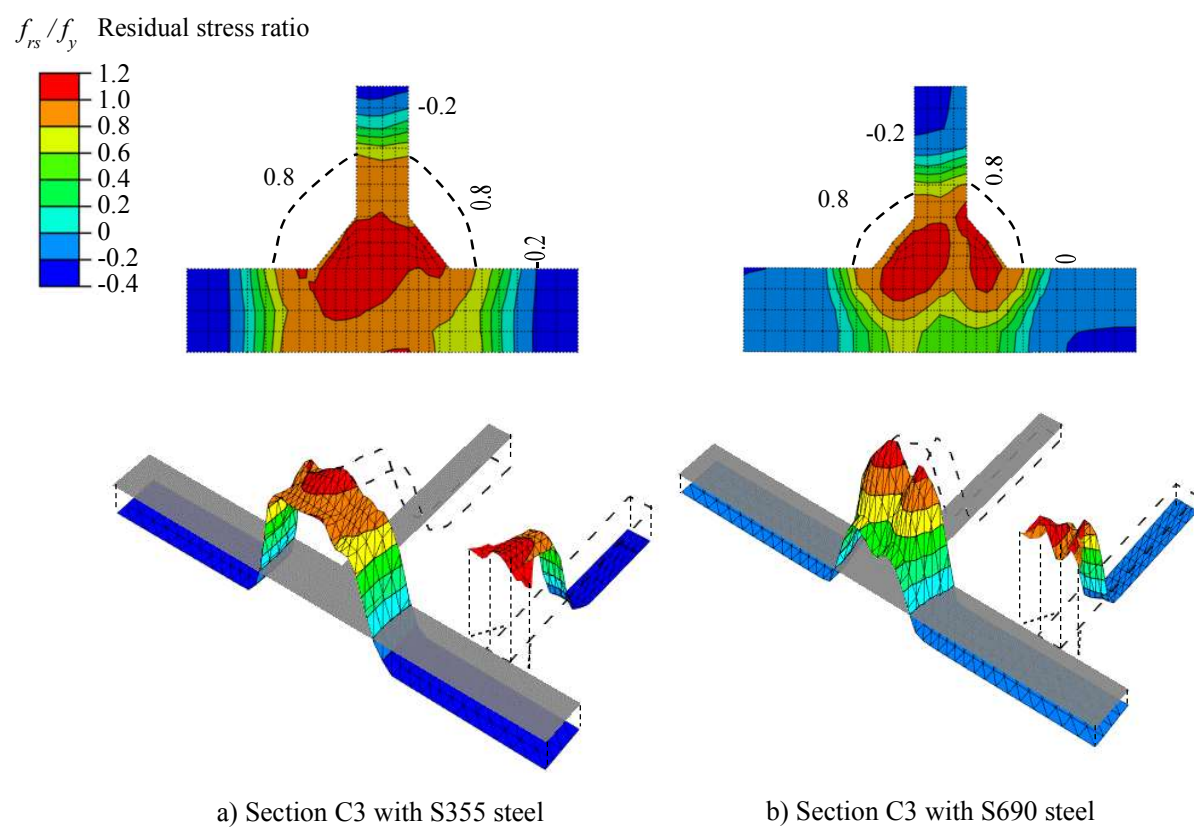
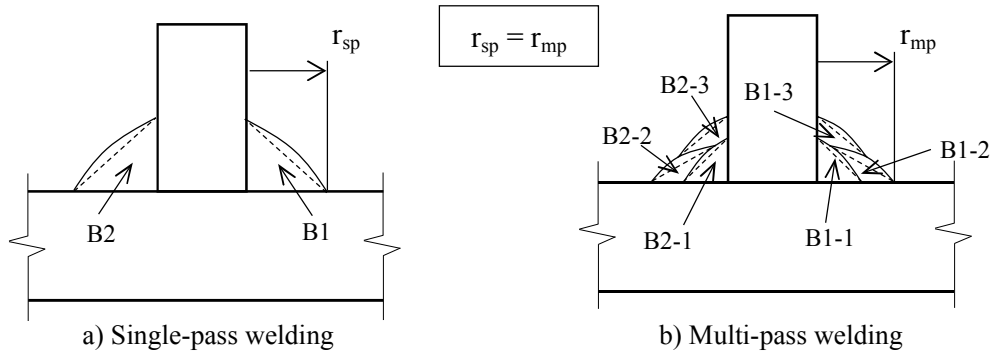


**Figure 10. Residual stress distributions of 2D models of S355 and S690 welded H-sections  
- Single pass welding**





Sections	Heat input energy (kJ/mm)	
	Single-pass welding	Multi-pass welding
C1 and C2	1.05	0.35
C3 and C4	2.00	0.67

**Figure 11. Welding runs in single-pass and multi-pass welding**

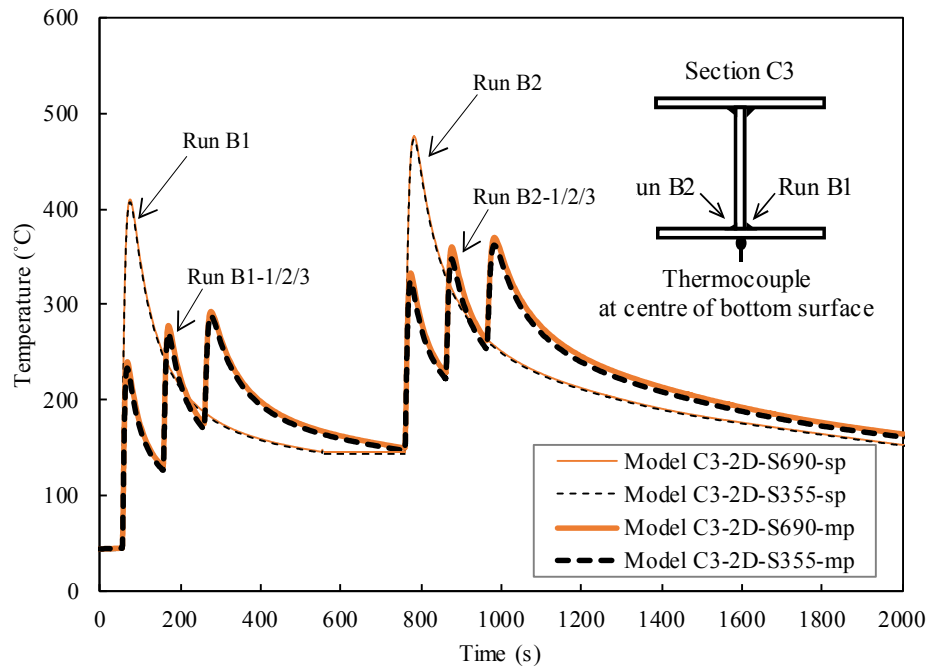
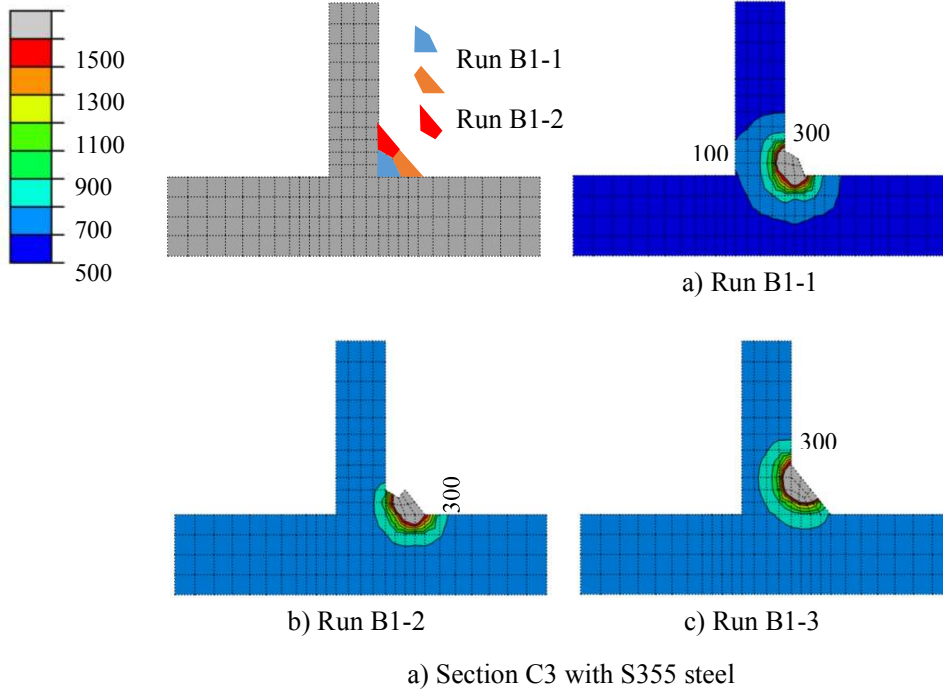


**Figure 12. Predicted temperature history of 2D models of welded H-sections - Multi-pass welding**

Temperature (°C) of **Run B1**



Temperature (°C) of **Run B1**

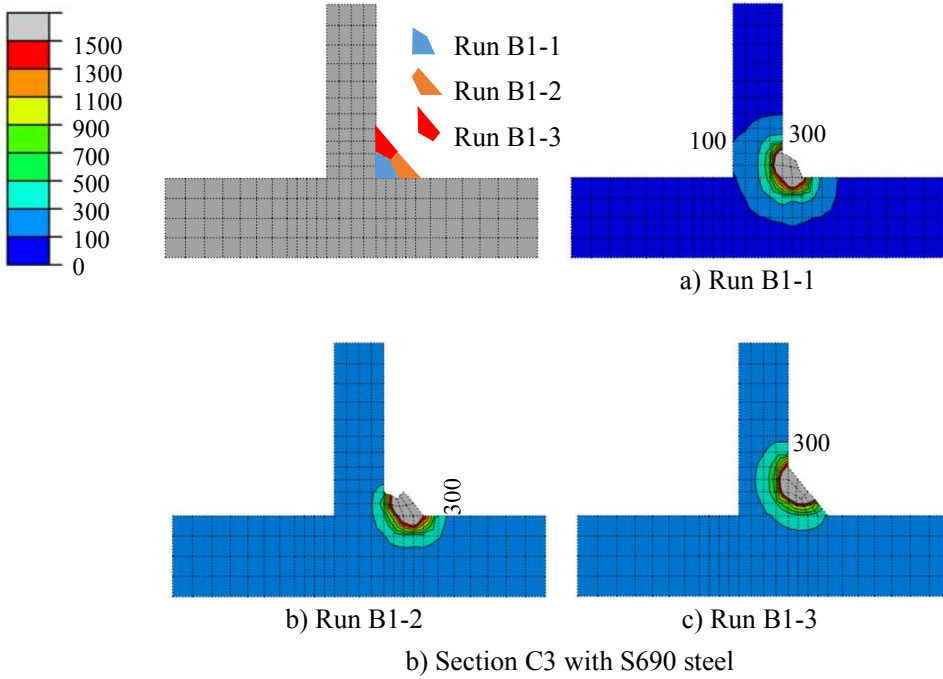
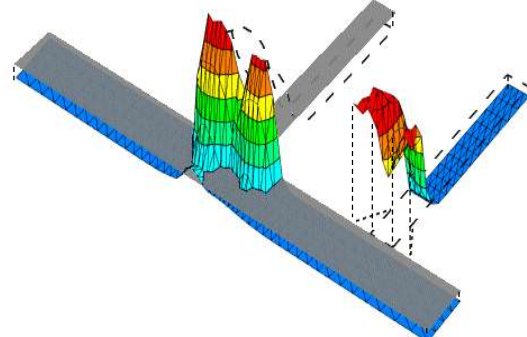
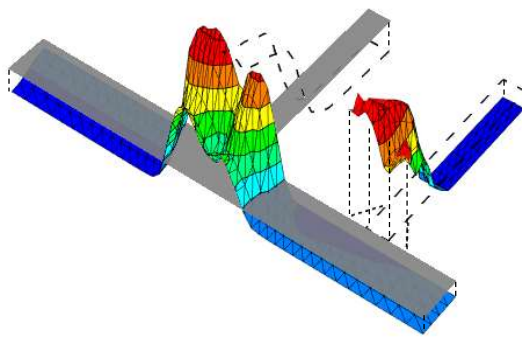
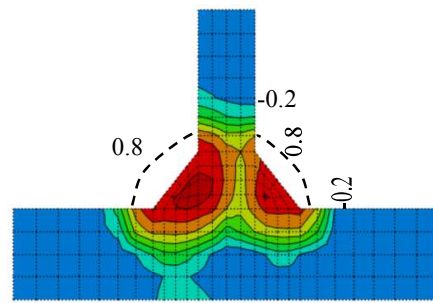
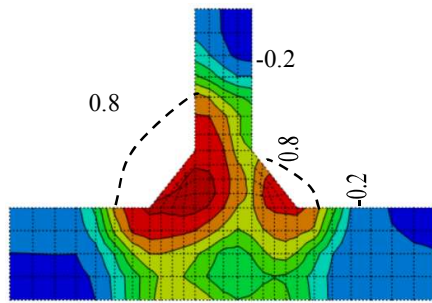
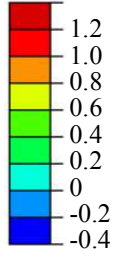


**Figure 13. Predicted temperature distributions of 2D models of S355 and S690 welded H-sections - Multi-pass welding**

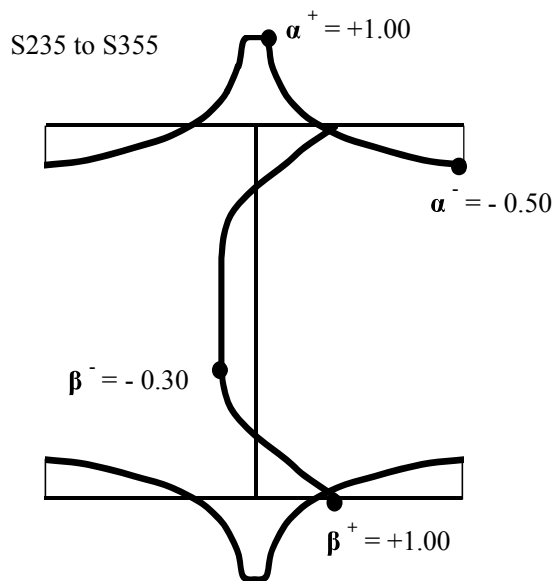
$f_{rs}/f_y$  Residual stress ratio



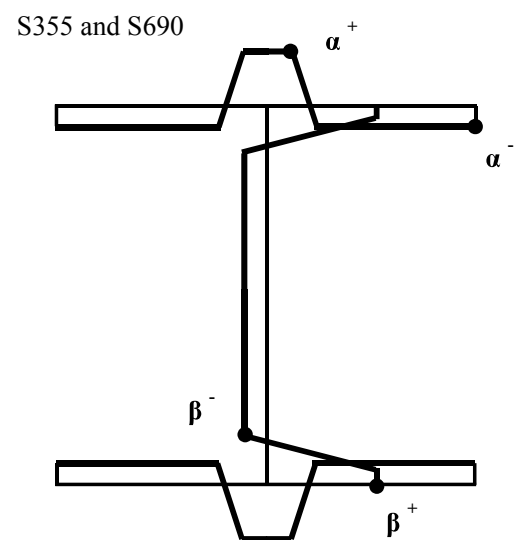
a) Section C3 with S355 steel

b) Section C3 with S690 steel

**Figure 14. Residual stress distributions of 2D models of welded H-sections  
- Multi-pass welding**



a) ECCS pattern



b) Proposed pattern

**Figure 15. Simplified residual stress pattern**

**Table 1. Residual stresses in 3D and 2D models of welded H-sections**

Steel grade	Model type	Section	Maximum residual stresses at outer surface (N/mm <sup>2</sup> )		Maximum residual stresses at inner surface (N/mm <sup>2</sup> )		Weighted average residual stresses within thickness (N/mm <sup>2</sup> )	
			Tensile	Compression	Tensile	Compression	Tensile	Compression
S690	3D single pass welding	C1	519	-239	928	-186	611	-204
		C2	532	-184	907	-141	618	-158
		C3	338	-154	902	-142	463	-120
		C4	399	-111	935	-101	455	-104
S690	2D single pass welding	C1	531	-214	889	-173	588	-181
		C2	544	-175	868	-145	588	-147
		C3	369	-147	915	-137	487	-134
		C4	373	-106	872	-103	487	-101

Notes: 1) Measured yield strengths are adopted.  
2) Weighted average residual stresses are given by  $\Sigma (A_i \times \sigma_i) / \Sigma A_i$  where  $A_i$  is the area of each element, and  $\sigma_i$  is the residual stress of each element.

**Table 2. Force equilibrium in 3D and 2D models of welded H-sections (Force in kN)**

Model type	Section	Flange			Flange/web junction		Web		Out-of-balance force		
		$F_{tf}$	$F_{c1f}$	$F_{c2f}$	$F_{t1,weld}$	$F_{t2,weld}$	$F_{tw}$	$F_{cw}$	$\Sigma F_t$	$\Sigma F_c$	$\Sigma F_t - \Sigma F_c$
3D	C1	+146	-91	-90	+16	+16	+53	-51	+231	-232	-1
	C2	+140	-85	-84	+16	+15	+51	-46	+222	-215	+7
	C3	+201	-155	-151	+32	+30	+135	-90	+398	-396	+2
	C4	+243	-176	-175	+33	+32	+146	-105	+454	-456	-2
2D	C1	+141	-84	-85	+15	+15	+51	-49	+222	-218	+4
	C2	+133	-83	-83	+15	+14	+49	-44	+211	-210	+1
	C3	+211	-161	-160	+34	+32	+142	-95	+419	-416	+3
	C4	+260	-187	-186	+35	+34	+156	-112	+486	-485	+1

**Table 3. Computing time of numerical analyses on 3D and 2D models of welded H-sections**

Steel grade	Section	Computing time (hours)		Saving in computing time
		3D model	2D model	
S690	C1	85.1	1.3	98.5%
	C2	96.3	1.6	98.3%
	C3	200.9	2.1	99.0%
	C4	255.0	2.5	99.0%

Notes: Specifications of the desktop computer used in this study:

- 1) CPU: Core i7, 3.4GHz
- 2) ROM Memory: 16G

**Table 4. Parametric study of 2D models of S355 and S690 welded H-sections  
- Single-pass welding**

Steel grade	Section	Model type	No. of sequential passes in a fillet root	Area of each weld pass, $A_{weld}$ (mm <sup>2</sup> )	Line heat input, q (kJ/mm)
S355	C1	2D	1	21.0	1.05
	C2	2D	1	21.0	1.05
	C3	2D	1	40.0	2.00
	C4	2D	1	40.0	2.00
S690	C1	2D	1	21.0	1.05
	C2	2D	1	21.0	1.05
	C3	2D	1	40.0	2.00
	C4	2D	1	40.0	2.00

**Table 5. Residual stresses of 2D models of S355 and S690 welded H-sections  
- Single-pass welding**

Steel grade	Model type	Section	Maximum residual stresses at outer surface (N/mm <sup>2</sup> )		Maximum residual stresses at inner surface (N/mm <sup>2</sup> )		Weighted average residual stresses within thickness (N/mm <sup>2</sup> )	
			Tensile	Compression	Tensile	Compression	Tensile	Compression
S355	2D single pass welding	C1	332	-200	381	-121	353	-174
		C2	325	-171	384	-106	353	-144
		C3	354	-124	388	-113	355	-120
		C4	354	-110	384	-92	355	-107
S690	2D single pass welding	C1	481	-204	790	-165	538	-166
		C2	578	-171	775	-140	538	-141
		C3	445	-136	819	-117	420	-125
		C4	450	-97	771	-95	420	-96

**Table 6. Force equilibrium in 2D models of S355 and S690 welded H-sections  
- Single-pass welding (Force in kN)**

Steel grade	Section	Flange			Flange/web junction		Web		Out-of-balance force		
		$F_{tf}$	$F_{cl,f}$	$F_{c2,f}$	$F_{t1,weld}$	$F_{t2,weld}$	$F_{t,w}$	$F_{c,w}$	$\Sigma F_t$	$\Sigma F_c$	$\Sigma F_t - \Sigma F_c$
S355	C1	+111	-69	-67	+9	+8	+39	-30	+167	-166	+1
	C2	+116	-70	-69	+8	+8	+36	-31	+168	-170	-2
	C3	+217	-143	-143	+16	+16	+99	-63	+348	-349	-1
	C4	+238	-154	-150	+18	+16	+106	-75	+378	-379	-1
S690	C1	+129	-77	-78	+14	+14	+45	-43	+188	-184	+4
	C2	+122	-76	-76	+14	+13	+43	-39	+179	-178	+1
	C3	+193	-147	-146	+31	+29	+126	-84	+350	-349	+1
	C4	+238	-171	-170	+32	+31	+138	-99	+408	-409	-1

**Table 7. Parametric study of 2D models of S355 and S690 welded H-sections**  
**- Multi-pass welding**

Steel grade	Section	Model type	No. of sequential passes in a fillet root	Area of each weld pass, $A_{weld}$ (mm <sup>2</sup> )	Line heat input, q (kJ/mm)
S355	C1	2D	3	7.0	0.35
	C2	2D	3	7.0	0.35
	C3	2D	3	13.3	0.67
	C4	2D	3	13.3	0.67
S690	C1	2D	3	7.0	0.35
	C2	2D	3	7.0	0.35
	C3	2D	3	13.3	0.67
	C4	2D	3	13.3	0.67

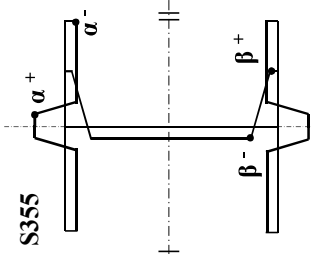
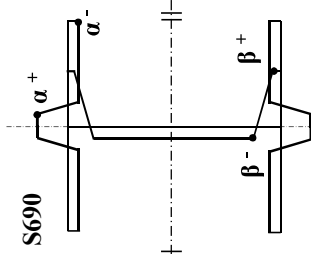
**Table 8. Residual stresses of 2D models of S355 and S690 welded H-sections**  
**- Multi-pass welding**

Steel grade	Model type	Section	Maximum residual stresses at outer surface (N/mm <sup>2</sup> )		Maximum residual stresses at inner surface (N/mm <sup>2</sup> )		Weighted average residual stresses within thickness (N/mm <sup>2</sup> )	
			Tensile	Compression	Tensile	Compression	Tensile	Compression
S355	2D multi pass welding	C1	245	-102	440	-77	259	-85
		C2	277	-88	429	-69	259	-78
		C3	284	-83	456	-59	249	-71
		C4	315	-72	449	-54	249	-64
S690	2D multi pass welding	C1	26	-105	788	-76	207	-86
		C2	74	-85	772	-73	207	-73
		C3	70	-79	833	-68	200	-68
		C4	108	-74	827	-58	200	-66

**Table 9. Force equilibrium in 2D models of S355 and S690 welded H-sections**  
**- Multi-pass welding (Force in kN)**

Steel grade	Section	Flange			Flange/web junction		Web		Out-of-balance force		
		$F_{t,f}$	$F_{c1,f}$	$F_{c2,f}$	$F_{t1,weld}$	$F_{t2,weld}$	$F_{t,w}$	$F_{c,w}$	$\Sigma F_t$	$\Sigma F_c$	$\Sigma F_t - \Sigma F_c$
S355	C1	+52	-34	-34	+8	+7	+26	-23	+93	-91	+2
	C2	+62	-40	-38	+8	+7	+26	-26	+103	-104	-1
	C3	+138	-88	-87	+15	+13	+70	-60	+236	-235	+1
	C4	+158	-100	-95	+15	+13	+74	-65	+260	-260	0
S690	C1	+39	-41	-40	+15	+14	+37	-26	+105	-107	-2
	C2	+46	-45	-45	+15	+14	+37	-28	+112	-118	-6
	C3	+110	-104	-101	+30	+29	+91	-56	+260	-261	-1
	C4	+125	-112	-110	+31	+30	+103	-68	+289	-290	-1

Table 10. Simplified residual stress patterns of S355 and S690 welded H-sections

Simplified pattern	Position	Single-pass welding				Multi-pass welding			
		Section C1	Section C2	Section C3	Section C4	Section C1	Section C2	Section C3	Section C4
 S355	$\alpha^+$	+1.00	+1.00	+1.00	+1.00	+0.73	+0.73	+0.70	+0.70
	flange								
	$\alpha^-$	-0.49	-0.40	-0.34	-0.30	-0.24	-0.22	-0.20	-0.18
	web								
 S690	$\alpha^+$	+0.78	+0.78	+0.61	+0.61	+0.30	+0.30	+0.29	+0.29
	flange								
	$\alpha^-$	-0.24	-0.20	-0.18	-0.13	-0.12	-0.11	-0.10	-0.10
	web								
	$\beta^+$	+1.00	+1.00	+1.00	+1.00	+0.92	+0.92	+0.92	+0.92
	$\beta^-$	-0.24	-0.20	-0.18	-0.13	-0.12	-0.11	-0.10	-0.10

Note: Refer to Tables 4 and 7 for details of single-pass and multi-pass welding.

**Table 11. Maximum residual stress ratios in the flanges and the webs of welded H-sections**

Steel grade	Position		Single-pass welding	Multi-pass welding
S355	Flange	$\alpha^+$	1.00	$-0.0003 \cdot b + 0.765$
		$\alpha^-$	$0.0014 \cdot b - 0.640$	$0.0004 \cdot b - 0.280$
	Web	$\beta^+$	1.00	0.92
		$\beta^-$	$0.0013 \cdot h - 0.647$	$0.0003 \cdot h - 0.281$
S690	Flange	$\alpha^+$	$-0.0016 \cdot b + 0.983$	$-0.0001 \cdot b + 0.321$
		$\alpha^-$	$0.0008 \cdot b - 0.326$	$0.0002 \cdot b - 0.149$
	Web	$\beta^+$	1.00	0.92
		$\beta^-$	$0.0007 \cdot h - 0.329$	$0.0002 \cdot h - 0.150$

Notes:

1.  $b$  is the flange width of the welded H-section (mm); and  
 $h$  is the section height of the welded H-section (mm).
2. Limits of applicability on geometrical dimensions of welded H-sections:
  - i.  $100 \leq b \leq 250$
  - ii.  $100 \leq h \leq 300$
  - iii.  $6 \leq t_w \leq 10$   
 $10 \leq t_f \leq 16$   
 $(t_f \approx 1.6 t_w)$